



RECENT EXPERIENCE AND INNOVATIVE APPROACHES IN DESIGN AND ASSESSMENT OF BRIDGES

Gian Michele CALVI¹

SUMMARY

Progress in design and assessment methods for bridge structures traditionally followed major earthquakes, where new evidence in damage and collapse became evident. This state of the art paper moves from a critical review of this logical process, emphasizing its progressive evolution from acting force and strength, to ductility capacity and demand, to displacement – based approaches. The most recent experience in bridge design and assessment is then discussed, enlightening some controversial or often neglected aspects, related to seismic input, response and design issues. Vertical input and axial force variation, soil structure interaction, appropriate application of capacity design principles, conceptual design of isolation systems.

INTRODUCTION

Design for strength (elastic design)

Bridges have been designed by reference to acceleration response spectra for the past 40 years. The reasons appear to be historical: engineers have always been more comfortable designing for “loads” such as self-weight, traffic loads, wind load, and river flow forces, than for deformation-inducing actions, such as temperature effects, creep and shrinkage, and earthquake actions. In the 1930’s, when new structures were first routinely designed for earthquakes, the parallel was with design for wind forces. Structures were designed to remain in the elastic range for a constant fraction of the gravity weight, applied as a uniform lateral force. It is well known [1, 2, 3, 4] that the consequences of this elastic design approach were severe underestimations of seismic deflections, inadequate combinations of action patterns produced by gravity and earthquake (due to the artificially low seismic forces) that resulted in mislocating points of contraflexure, premature termination of reinforcement etc., and neglecting of any detailing capable of favoring large inelastic deformation without significant strength degradation.

The consequences in terms of damage and collapses of bridges are also well known, and will not be repeated here.

¹ Professor, Università degli Studi di Pavia, and Director, European Centre for Training and Research in Earthquake Engineering, Pavia, Italy. E-mail: gm.calvi@unipv.it

Design for ductility (strength design)

As understanding of the dynamic characteristics of seismic structural response became more general in the 1950's and 1960's, and as it became realized that structures survived levels of response accelerations that apparently exceeded those corresponding to the ultimate strength, the concept of "ductility" was adopted. This was an attempt to reconcile inconsistencies in the fundamental basis of force-based design, attributing to the capacity of a structure to deform inelastically without significant strength loss the reason for surviving an earthquake that would have required more strength than that available to respond elastically.

Concepts and rules to relate ductility and some kind of "equivalent strength" were developed by a number of researchers (e.g. [5]), developing the well-known concepts of conservation of acceleration, velocity and displacement as a function of the fundamental period of vibration of the structure.

Most codes of practice are still based on these concepts. Essentially, elastic acceleration spectrum are reduced as a function of an assumed ductility capacity of bridges, and "capacity design principles" [6] are applied to assure that the assumed post elastic mechanism will develop, avoiding potential brittle damage modes.

Design for displacement

Even in the present time, with a variety of new design approaches that require increased emphasis on displacement, rather than on strength, the most common approach has been to attempt to modify force-based design procedures, rather than to completely revise seismic design procedure in a more rational manner.

The assumption that an elastic acceleration spectrum provided the best means for assessing the seismic response of a structure has been proven to be a fallacy [7, 8] on the base of the following points:

- Design ignores duration effects and condenses response into "snapshots" of transient behavior at maximum modal response. These modal maxima are combined by modal combination rules of dubious relevance for inelastic structural response. It is assumed that maximum transient response is more relevant than the final "at rest" condition of the structure after the earthquake, which is not considered in the design process.
- It is generally accepted that damage can be related to material strains, and that material strains can be related to maximum response displacements, but not to response accelerations. It would thus seem important for design procedures to emphasize the importance of estimating peak displacement response, which is evaluated quite differently according to different approaches and codes. The normal approach involved modification of the displacements of the corresponding elastic system of equal initial stiffness and unlimited strength, possibly assuming the equal displacement approximation, thus estimating the design displacement as:

$$\Delta_{\max,duct} = \Delta_{\max,elastic} = \frac{T^2}{4\pi^2} \cdot a_{(T)}g \quad (1)$$

The equal displacement approximation is known to be non-conservative for short-period structures. If the equal energy approach is applied, equating the energy absorbed by the inelastic system, on a monotonic displacement to peak response, to the energy absorbed by the equivalent elastic system with same initial stiffness, the peak displacement of the inelastic system is:

$$\Delta_{\max,duct} = \Delta_{\max,elastic} \cdot \left(\frac{R^2 + 1}{2R} \right) = \frac{T^2}{4\pi^2} \cdot a_{(T)}g \cdot \left(\frac{R^2 + 1}{2R} \right) \quad (2)$$

where R is the design force-reduction factor.

According to the UBC [9], the design displacements was estimated as:

$$\Delta_{\max,duct} = \Delta_y \cdot \frac{3R}{8} \quad (3)$$

hence:

$$\Delta_{\max,duct} = \Delta_{\max,elastic} \cdot \frac{3}{8} \quad (4)$$

Priestley [8] showed that all formulations are correct at some part of the period range of structural response, and all are wrong at other periods. This was explained with reference to typical displacement spectra, reproduced in figure 1, where the influence of inelastic response was represented by a lengthening of the effective period of response, with hysteretic damping being represented as equivalent viscous damping. For short period structures, the increase in displacement response from period elongation is less than the decrease resulting from increased damping. For medium period structures, the two effects almost balance each other. For long period structures the period elongation does not result in significant displacement increase, and the influence of increased damping is to reduce the overall displacement response. For very long period structures, the displacement is equal to the ground displacement, independent of period and damping.

- It was also noted [8] that the elastic acceleration approach placed excessive emphasis on the elastic stiffness characteristics of the structure and its elements. For reinforced concrete and masonry structures the estimation of these stiffness values varies greatly between different design codes. Further, these elastic characteristics only pertain to low level seismic response, and are permanently modified as soon as the structure exceeds yield.

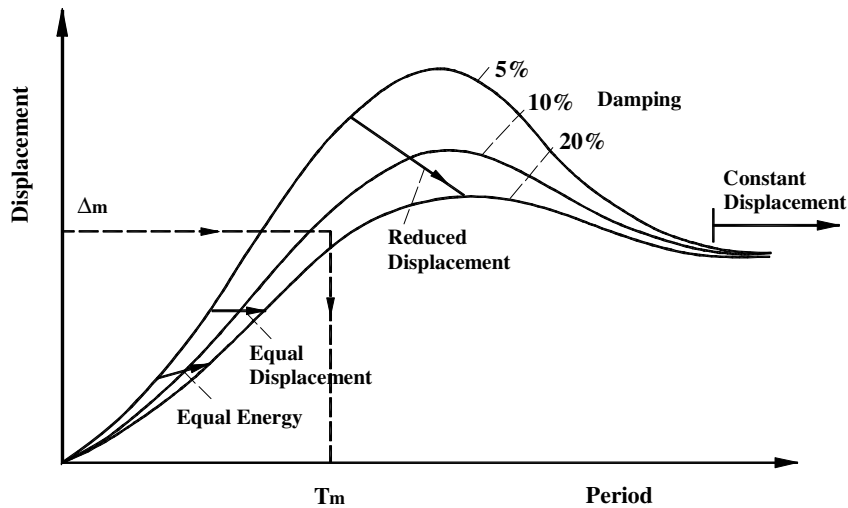


Fig. 1 Displacement spectra for different levels of damping

A number of displacement-based (some times referred to as performance-based) design methods were developed [10]. In general, and more specifically in one of the approaches [11], the fundamental difference from force-based design is that the structure to be designed is characterized by a single-degree-of-freedom (SDOF) representation of performance at peak displacement response, rather than by its initial elastic characteristics. This is based on the *Substitute Structure* approach [12, 13].

The design approach attempts to design a structure which would achieve, rather than be bounded by, a given performance limit state under a given seismic intensity, essentially resulting in uniform-risk structures, which is philosophically compatible with the uniform-risk seismic spectra incorporated in most design codes. The design procedure determines the strength required at designated plastic hinge locations to achieve the design objectives in terms of defined displacement objectives. It must then be combined with capacity design procedures to ensure that plastic hinges occur only where intended, and that non-ductile modes of inelastic deformation do not develop.

RECENT EXPERIENCE

Design of the Rion – Antirion cable stayed bridge [14, 15]

Description of the bridge

The Rion Antirion bridge is located in Greece, between the Peloponese and the continent, over the Gulf of Corinth. The structure will span a stretch of water of some 2500 m with a depth between 60 and 70 m. No bedrock has been encountered during soil investigations down to depth of 100 m; the sediment depth has been estimated around 500 m; the soil profile is rather heterogeneous, with strata of sand, silty sand, silty clays and clays.

The 2000 years return period design earthquake has been defined by peak ground acceleration equal to 0.48 g and a response spectrum with a maximum amplification plateau at 1.2 g between 0.2 and 1.0 s. The main part of the bridge consists of three central cable stayed spans of 560 m and two side spans of 286 m, for a total of 2252 m (fig. 2).

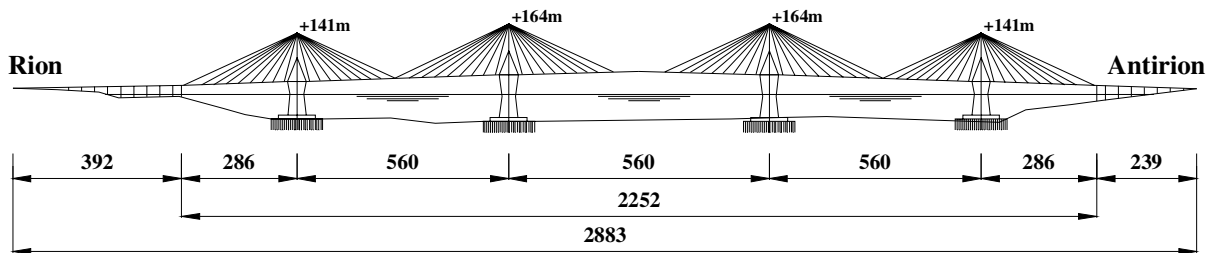


Fig. 2 Elevation of the Rion Antirion bridge

Dynamic modal analysis

Modal analyses of the structure were performed independently by designers and checkers. In case of a full model, at least 500 modes had to be considered to obtain a total mass participating around 85%. The first modes were typical pendulum modes; the first one had a period of vibration around 7.5 s. The first mode that implied a significant participation of the pier mass was around the 260th, with a period of vibration around 0.6 s. All these essential results were also captured by strongly simplified models.

Capacity designed foundations

The foundations are large diameter (90 m) caissons resting on the seabed, where the upper layers have been reinforced with hollow steel pipes, 25 to 30 m long, with a diameter of 2 m, spaced at 7 m distance. Between the top of these inclusions and the base of the foundation, a 3 m thick gravel layer has been inserted, with the purpose of creating a potential sliding surface capable of limiting the shear force transmitted between soil and structure. A fundamental objective of the design was to avoid failure mechanisms involving large rotations, producing extremely large displacements in the high rise pylon, in favor of sliding failure modes, in which case the permanent displacements are of the same order of magnitude along the height of the structure.

This is clearly more important than the limitation of shear forces, since the structural response was not significantly different in case of linear or non-linear modeling of the soil.

Effects of soil – structure interaction and non – synchronous input

The assumption of lower, intermediate or upper bound characteristics for the soil response had very significant effects on the structural response; in case of lower bound soil the displacement

demands were normally in the range of three times those in case of upper bound soil, with peak values in the range of 4 m between fixed soil and top of the tower.

On the contrary, the simulation of traveling effects of the seismic waves had little effects on all design parameters, such as relative displacement demands and variation of forces in the pylon legs.

Deck displacement control devices

The cable-stayed deck is fully suspended and behaves like a damped pendulum. Four hydraulic dampers with a capacity of 3,500 kN each are connecting each pier head and deck, in addition to a sacrifice steel strut connector, with a 10,000 kN capacity, designed resist winds and ordinary horizontal forces, but to break in case of a strong earthquake.

The selection of the characteristic of the damping system was based on extensive numerical analyses, aimed to define the optimal compromise between relative displacement demand between deck and pier and level of shear to be transmitted. In case of assumption of lower bound soil properties, as pointed out by far the most demanding, the force demand with fixed connection was in the order of 70 MN, the displacement demand without connection in the order of 3 m. The use of hydraulic dampers should allow a limit force up to 14 MN, with displacements around 2 m and velocities around 1.5 m/s.

Displacement capacity for high axial force

Each pylon is composed of four square legs, with side of 4 m, joined at the pier head to form a monolithic structure where the cables are anchored. The configuration with four legs obviously induce a potential for a vertical stress in one leg larger than four times the gravity stress, since three legs can go into tension. This potential for a high axial stress strongly reduces the ductility and displacement capacity of the leg, where a potential formation of plastic hinge is considered in case of strong earthquake. As a consequence, the gravity stress had to be kept considerably low. The relative displacement demand was estimated around 0.75 m in case of lower bound soil, compatible with the displacement capacity in case of a gravity axial load ratio of approximately 0.1, resulting in a maximum axial load ratio during the design earthquake around 0.5.

Assessment and strengthening of the Bolu viaduct [16]

Description of the original structural configuration

Bolu Viaduct 1, part of the Great Anatolian Highway, consists of two parallel bridges, each carrying a separate traffic direction, with the Ankara-bound bridge (right bridge) having 58 spans, and the Istanbul-bound bridge (left bridge) having 59 spans. Each span is approximately 39.4m long, and is constructed from 7 precast V-girders with an in – situ topping. Each span was supported on pot-bearings designed for 200mm maximum travel. A 1.5m long link-span extension of the deck slab connected the spans into 10-span segments with movement joints between the 10-span segments. However, because of the bearing support detail, the gap between the girder ends, and the flexibility of the link-slab, the spans remained effectively simply supported for live loads as well as dead loads.

At internal supports, the bridge is supported by tall hollow reinforced concrete piers of approximately rectangular section modified by architectural detailing, generally in the range 40-50m high, though a number of shorter piers exist, particularly near the Istanbul abutment.

Piers are founded on massive reinforced concrete pile caps, in turn supported on twelve 1.8m diameter Cast-In-Drilled-Hole (CIDH) piles passing through superficial soils of variable strength and bearing on alluvium layers, generally at about 30m depth.

At the bridge ends, the V-girders were individually supported by pot-bearings on a seat-type abutment, again supported on CIDH piles, but of reduced number and size.

Seismic resistance relied primarily on a seismic isolation system consisting of “crescent-moon” steel energy dissipating units (EDU’s) located at each support connecting the spans to a centrally mounted dissipator support block. At movement joints and the central pier of each 10-span segment, the EDU’s incorporated sliders and lock-up pistons to allow relative thermal movements to occur freely, but to ensure full engagement of all EDU’s under seismic loading. Displacement capacity of the EDU’s was 480mm. Transverse displacements were restrained by shear blocks adjacent to beams 3 and 5 as a back-up in the event of extreme displacements, and longitudinal relative movements at expansion joints were constrained by cable restrainers.

Damage summary

On November 12, 1999 an earthquake of moment magnitude 7.2 occurred on the Duzce fault causing severe damage to tunnels and bridges under construction on the Great Anatolian Highway [17]. Peak ground accelerations in the vicinity of 0.8g, based on accelerograms recorded nearby were estimated at the viaduct site. More important to the bridge performance, right – lateral fault slip of approximately 1.6m occurred on a fault scarp traversing the bridge alignment, at an acute angle (approximately 15 degrees to the bridge longitudinal axis), resulting in shortening of the bridge length by about 1.5m, concentrated over two spans of the bridge.

Displacements resulting from the fault slip and the vibratory response exceeded the capacity of the seismic isolation system. As a consequence, the EDU’s were destroyed, and the pot-bearings at most beam ends were ejected. Impact between the ends of the central V-beam and the EDU support block occurred at most spans, destroying many of the support blocks and damaging many of the beam 4 ends. In most cases the damage to beam ends was superficial, though in one case the damage included crushing of concrete and fracture of reinforcement for a distance of up to 4m from the beam support.

Impact between the transverse shear restraint blocks and beams 3 and 5 caused extensive damage to the shear blocks, and some damage to beam ends, though this was superficial. Further damage to beam ends, applicable to all beams across the section, occurred as a consequence of unseating from the pot-bearings, with impact between the beam end and the bearing support block, or the pier cap. This damage is minor in all cases.

As a consequence of the fault movement and the failure of the EDU’s, residual displacement of the beam ends was considerable, being as high as 1100 mm longitudinally, and 500 mm transversely. In a number of cases this displacement was such that the beam ends remained unsupported, hanging over the edge of the pier cap. In such cases, and where the beams ends were unsupported (having moved beyond the edge of the bearing blocks) but were still within the plan area of the pier cap, support for the beam end was only provided by flexure of the link span joining adjacent spans. The factor of safety against failure in these cases, using conventional flexural strength theory, is less than 1.0, since the shear corresponding to flexural strength of the link slab is only 90% of that needed to support the reaction of the span dead-load, using expected (rather than nominal) material properties, and ignoring strength reduction factors. It will also be noted that during unseating of the beam ends, the shear in the link spans will have been increased by dynamic impacts, to perhaps twice the static value. It is apparent that catastrophic failure has been averted by large vertical relative displacements, up to 300mm, which have occurred across these 1800mm long link spans, and the strength is apparently provided by a combination of flexure and tensile tie action in the link slab reinforcement, aided by the side fascia panels, which are deeper than the link span.

Shortening of the bridge length as a consequence of the fault slip has largely been accommodated by reduction in the distances across the movement joints. Note that the movement joints had not yet been installed when the earthquake struck.

At the abutments, damage is similar to that at internal supports, being largely confined to EDU support blocks, transverse shear restraint blocks and beam ends. However, additional damage was caused to abutment back walls by impact as the bridge was driven towards Istanbul.

The hollow reinforced concrete pier stems were largely undamaged, though a number of piers have small but significant tilts or rotations, particularly where the fault crossed the bridge. Some piers have twisted about the vertical axis by approximately 4 degrees.

With six exceptions, damage to the foundations is minor. Damage to the six exceptions include significant pile cap cracks, and plastic hinging to the piles, as a consequence of gross ground displacements in the vicinity of the fault movement. Where the foundations were rotated by proximity to the fault, damage to the piles was severe.

Displacement demand and near fault effects

Intensive site and theoretical seismological investigations indicated that the redesign input ground motion should be characterized by the following properties, characteristic of a 2000yr return period ground motion [18]:

- Design peak ground acceleration (PGA) 0.81g
- Design peak spectral acceleration (5% damping) 1.8 – 2.0g
- Design peak spectral displacement (5% damping) 600mm
- Consideration of near field directivity effects.

The latter point meant that fling effects (velocity pulses) and fault slip should be considered. A ground permanent deformation of up to 500 mm was estimated to be possible during the design life of the bridge (an average of 5 mm per year over a period of 100 years). Any design action to be considered for the analysis of the viaduct should therefore be based on these assumptions, and in addition should try to satisfy the following conditions, which characterize the Duzce fault and the location of the viaduct:

- The magnitude of the earthquake should be of the order of 7-7.2;
- The earthquake fault rupture should be strike slip;
- The recording site should be located with respect to the epicenter in such a way that the angle between the fault and the line connecting epicenter and location is clockwise and small.

With the fault locked until fracture occurs, the question arises as to how will the fault movement be distributed with distance from the fault (which passes through the bridge). Clearly two points some kilometers away from the fault on either side will move relatively by the fault movement, but two points a few meters on either side of the fault will essentially experience no relative movement until the fault ruptures. On the other hand, the two points close to the fault will experience the full fault dislocation during the fault rupture as an essentially instantaneous relative displacement, whereas the two points kilometers from the fault will see no additional relative displacement during the fault rupture.

If the relative displacement develops rapidly with distance from the fault (say within a few spans of the bridge from the fault), then most of the pier/bearing systems will need to be designed to accommodate the additional displacements due to tectonic movement. However, if the tectonic displacements develop only slowly over a number of kilometers from the fault, then until the fault fractures, the piers of the bridge will maintain their current relative locations as tectonic movements develop. When the fault ruptures, relative displacements will develop only in the immediate vicinity of the fault, affecting bearings in the immediate vicinity.

Both theoretical considerations and measurements of relative displacements of the pier bases supported slow development of tectonic relative displacement with distance from the fault, indicating that the abutments moved closer together by an amount at least equal to the fault dislocation of 1.5 m. This could not have happened if the ground at the abutments had already been displaced by the full (or a significant part of) the relative tectonic displacement. As a consequence only a small number of piers would need to be designed to accommodate the sum of vibrational and dislocation displacements.

It could also be argued that it is unlikely that full vibrational and dislocation displacements will be additive, as it implies that (a) the dislocation occurs before the vibrational peak (which may be possible, but is uncertain), and (b) that the vibrational response, which is dependent on the development of resonance, is unaffected by the fault dislocation. It would seem probable that the process of fault

dislocation would act to damp out vibrational response. As this controversial issue could not be resolved with certainty, the bearings in the vicinity of the fault are to be designed for the full combination of vibration and dislocation.

Deck continuity

It was immediately apparent that the existing detail for supporting the simple spans on the pier heads would not provide adequate displacement capacity and that continuity over supports would be necessary. Preliminary redesign focused on making the 10-span bridge segments fully continuous and using reduced numbers of large capacity (axial force and displacement) seismic isolation bearings. The process of creating continuity involved casting a new prestressed diaphragm beam at each internal support, of sufficient width to capture the end 600mm of the beams of the two adjacent spans. Longitudinal continuity between the beams and the new diaphragm beams was achieved partly by shear friction, based on the effective prestressed force, and partly by dowels drilled into the beam end and side faces. At internal supports, the diaphragm width is 3.6m, resulting in a significant additional mass to the superstructure (about 10%). Two isolation bearings would be inserted between the diaphragm and the pier head. Placing the diaphragm beam results in very little difference to the way dead load is supported. Live loads are supported by fully continuous action, well within the shear friction capacity of the beam/diaphragm connection. The critical design case for the connection was found to be differential thermal effects resulting from diurnal temperature fluctuations in midsummer. At movement joints, separate prestressed diaphragm beams of reduced width were provided at each segment end.

Pier and isolation systems

Normally it can be assumed that force levels can be kept to a desired maximum level by seismic isolation, at the penalty of increased displacements. In the case of the Bolu viaduct, however, the mass of the piers is typically larger than that of the superstructure, as a consequence of the tall piers, and short spans (20.5MN compared with 14MN for the tallest piers). With a seismic isolation system placed between the superstructure and the pier head, only the superstructure mass is isolated, and pier moments resulting from pier self-mass are unreduced. As the seismic intensity increases, the pier moments and shears must therefore also increase.

A second concern with seismic isolation was the level of displacement that might develop between deck and pier head. In the normal seismic isolation approach, bearing displacements will be less than the 5% spectral displacement for the isolation period, as a consequence of structure flexibility and additional damping provided by the isolation system. The displacements would be much less than the peak 5% spectral displacements. However, with the high pier mass, the response is essentially a two-mass system, and in the second mode the pier head and the superstructure move out of phase. In this case the bearing displacement can be significantly higher than the spectral displacement for the second mode period. Also, it was clear that the argument related to the first mode, expounded above, was a simplification, since the high mass of the pier would result in the effective height being some distance below the superstructure, and hence the bearing displacement could still exceed the spectral displacement in the first mode alone.

On the contrary, the displacement capacity of the taller piers would exceed the maximum that could possibly develop in the design level intensity. Actually, Moment-curvature analyses were carried out to determine capacities corresponding to different limit states, using material strength data recorded during construction, and without using strength reduction factors. The results of these analyses indicated nominal shear capacities in excess of nominal moment capacities and longitudinal and transversal displacement capacities at the serviceability limit state exceeding 1.0 m and 0.6 m respectively for pier heights greater than 40m (about 90 % of the cases).

A third concern was related to the specific kind of devices selected by the client, i.e. friction pendulum isolation bearings, for which an appropriate consideration of axial force variation effects may be needed [19]. These effects may not be significant for what concerns variation of the displacement demand, but may induce important increment of shear, bending and torsional moment demand on the piers. For the

case of the Bolu viaduct, however, the fundamental parameters that may amplify, or reduce, these effects are rather favorable, as discussed below.

- Ratio between deck and pier mass: a significant variation of the shear force transmitted from the deck to the pier may result in strongly attenuated effect at the pier base when the ratio of the pier mass to the deck mass is high. This is clearly the case for the Bolu viaduct.
- Aspect ratio of the deck: for the same level of horizontal force, the axial force variation possibly induced by the horizontal acceleration is higher for a deck section relatively larger and for devices relatively closer one to each other. The case of Bolu is again favorable, with a ratio between bearing distance and horizontal forces couple around 5.
- Radius of curvature of the viaduct: a curved bridge may result in higher effects, due to the interaction of vertical and horizontal response. The Bolu viaduct is relatively straight.
- Intensity of the ground motion: relatively high horizontal peak ground accelerations may induce more significant effects, like in the present case, where a PGA in excess of 0.8 g is assumed.

The results obtained from the analysis generally confirmed what was intuitively expected, and were reassuring for what concerns the response of the Bolu Viaduct.

ASPECTS RELATED TO SEISMIC INPUT AND RESPONSE

Acceleration and displacement spectra

Acceleration spectra

As discussed, acceleration spectra are the basic kind of representation of the seismic input when strength and ductility are the fundamental design parameters. Several reasons to believe that acceleration spectra do not represent the best means to assess the seismic response of a structure have been discussed in the introduction and will not be repeated here.

However, it has to be noted that additional concerns may arise for the case of bridges, and in general for structure characterized by long periods of vibration. Actually in this case acceleration spectra are characterized by relatively low levels of acceleration and design may be based on minimum levels rather than by a proper estimate of the demand. The possible presence of strong pulses, typical of near fault action (discussed later) may have a moderate impact on the spectral shape [20]. On the opposite, it has to be recognized that large displacement demand are typical of long period structures, and near fault effects have a tremendous impact on this parameter.

This evidence points towards the use of displacement spectra as a better way to represent the design action.

Displacement spectra

It is well known [11] that design displacement spectra for a given level of damping, say for example 5%, can be generated from the acceleration spectra using the approximate relationship

$$\Delta_{T,5} = \frac{T^2}{4\pi^2} \cdot a_{T,5}g \quad (5)$$

where $\Delta_{(T,5)}$ and $a_{(T,5)}$ are the response displacement and acceleration coefficient for period T and 5% damping.

Recent work [21, 22] has enabled [11] to generate approximate elastic displacement spectra for strike-slip earthquakes of different magnitudes. The spectra are characterized by a linear increase in response displacement with increasing period, followed by a plateau. At high periods the response displacement eventually decreases to the peak ground displacement, but this will rarely be of significance for bridge design (except, perhaps, suspension and cable-stayed bridges).

The corner period T_c between the linearly increasing and plateau part of the spectrum, and the maximum displacement δ_{\max} for firm ground can be related to the moment magnitude M_w by the following expressions:

$$T_c = 1.0 + 2.5(M_w - 5.7) \text{ seconds} \quad (6)$$

and

$$\delta_{\max} = \frac{10^{(M_w - 3.2)}}{r} \text{ (mm)} \quad (7)$$

where r is the nearest distance from the site to the fault plane in km. For rock and soft soil sites, the displacement given by Eq. (7) should be multiplied by 0.7 and 1.5 respectively to give approximate representation of soil conditions [23].

Equations (6) and (7) are plotted in figure 3 for different earthquake magnitudes, and for different distances from the fault plane. It should be noted that these apply for design spectra dominated by a single causative fault. The consequences in terms of the shape of uniform-risk spectral displacement shapes are less obvious than for specific earthquake intensities.

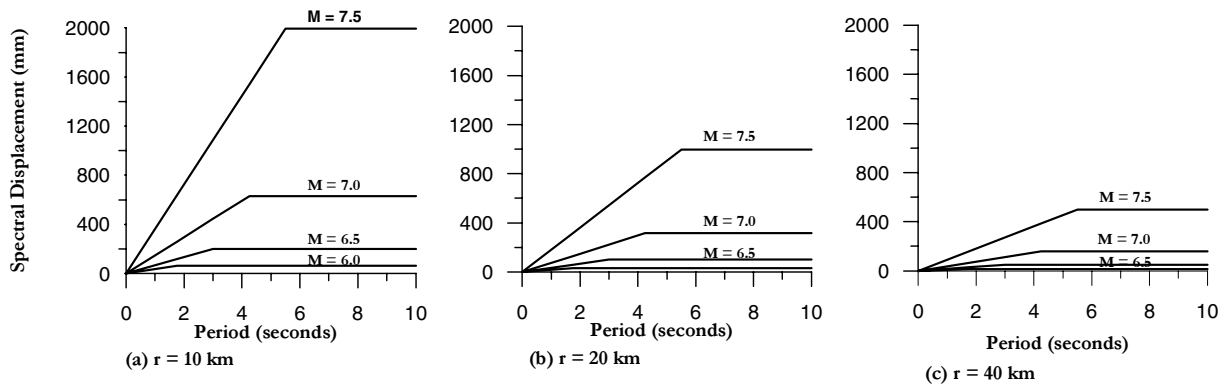


Fig. 3 Influence of Magnitude and Distance on 5% Damped Displacement Spectra [11]

Vertical component and axial force variation

The importance of the vertical seismic input in the structural response of bridges has been investigated by various authors [24, 25, 26]. The damaging effects of the vertical component are more evident in the near field since the vertical motion attenuates faster than the horizontal one: in this case ground motions from large earthquakes ($M_s > 7$) can produce significant horizontal and vertical components and the ratio of the vertical to horizontal maximum PGA may exceed 1.

The energy content of the vertical component is concentrated in a narrow high frequency range. This results in a possibly dangerous match with the vertical periods of common bridges, usually belonging to the higher frequency range. Furthermore, several records indicate that the maximum vertical response occurs 1 or 2 seconds earlier than transverse one, others show a coincidence in time. A compendium of field observations and analytical results indicates that certain failure modes are convincingly attributable to high vertical earthquake-induced forces, which, in addition to the possible overstressing in compression or tension, may induce shear or flexure failure. An increase in shear demand may be due to second order effects caused by the presence of high vertical dynamic forces.

The effects of axial force variations may be emphasized in presence of isolation systems. The case of friction pendulum systems (FPS, used for the upgrading of the Bolu viaduct, as discussed) offers an interesting example to discuss possible effects and consequences. FPS use geometry and gravity to achieve the desired isolated response, based on well-known principles of pendulum motion. Though,

friction pendulum systems may be strongly influenced by the axial load level acting at a given time, since a variation of the axial force results in corresponding variation of equivalent yielding level and in the post-yielding stiffness in the non-linear phase of the hysteretic response, and this, in turn may produce increments in the shear force demand and potential torsional effects on the piers.

The axial force variation on an isolation device is not only affected by the vertical acceleration, but also depends on a combination of effects due to horizontal input (because of the necessary dynamic equilibrium to the horizontal forces) and to the geometrical configuration (plan and elevation irregularities).

An extensive, though not conclusive, study on the subject [19], based on parametric non-linear time history analyses, showed that the inclusion of axial force effects may not be significant for what concerns variation of the displacement demand, but may induce important increment of shear, bending and torsional moment demand on the piers.

The fundamental parameters that may amplify, or reduce, these effects are the ratio between deck and pier mass, the aspect ratio of the deck, the radius of curvature of the bridge, the intensity of the ground motion and the consideration of vertical input, as briefly discussed below.

- Ratio between deck and pier mass: a significant variation of the shear force transmitted from the deck to the pier may result in strongly attenuated effect at the pier base when the ratio of the pier mass to the deck mass is high.
- Aspect ratio of the deck: for the same level of horizontal force, the axial force variation possibly induced by the horizontal acceleration is higher for a deck section relatively larger and for devices relatively closer one to each other.
- Radius of curvature of the viaduct: it is shown that a curved bridge may result in higher effects, due to the interaction of vertical and horizontal response.
- Intensity of the ground motion: relatively high horizontal peak ground accelerations may induce more significant effects.
- Consideration of vertical input: the inclusion of the vertical component of the input ground motion may result in being the crucial point to verify whether important effects have to be expected and considered.

These considerations may be of some help in deciding whether axial force effects may be neglected or should be considered in the analysis.

A fundamental aspect related to design concept should also be noted. Actually, when dealing with isolated bridges, it is common practice to assume that possible pier collapses are capacity protected by the shear capacity of the isolation system. This implies that there is no reason to protect a possibly brittle shear collapse mode with a lower strength flexural yielding of the pier. Clearly, this situation may not apply if a significantly higher shear force is transmitted from the deck to the pier. As a consequence, it is felt appropriate to recommend that when using friction pendulum systems capacity design principles are still applied to protect undesired failure modes of the pier and foundation system.

Near fault effects

Ground motion records from recent earthquakes confirmed that near fault ground motions are dominated by a large long period pulse of motion that occurs at on the horizontal component perpendicular to the strike of the fault. Preliminary equations to define appropriate response spectra, taking into account magnitude dependence of the pulse and rupture directivity effects have been proposed [20], but it appears that significant developments are needed before transferring these scientific findings into common practice. As described in relation to the case of the Bolu viaduct, permanent differential displacements may combine with strong pulses and directivity effects, resulting in anomalous demand.

With reference to displacement-based design approaches, it has been noted that the presence of a dominating single pulse in the ground motion results in a strongly diminished capacity of dissipating energy for the structure, and this may in turn results in larger displacement demand. Based on these

considerations, on the equation recommended in EC8 [23] to take into account different level of viscous damping and on the recognized equivalence between viscous damping and hysteretic energy dissipation, a modified correction factor has been proposed to evaluate the displacement demand in near fault conditions [8]. This proposal, described below, is based on empirical evidence and certainly needs validation and refinements, but has connotation of simplicity and applicability.

For normal accelerograms EC8 proposes the following expression to compute the displacements corresponding to a different level of damping, as a function of the displacement for 5% damping:

$$\Delta_{T,\xi} = \Delta_{T,5} \cdot \left(\frac{10}{5 + \xi} \right)^{0.5} \quad (8)$$

As discussed above, in the near-field region, the influence of velocity pulses may reduce the effectiveness of damping (and hysteretic energy absorption), therefore Eq. (24) is likely to be non-conservative, and may be replaced by the following one:

$$\Delta_{T,\xi} = \Delta_{T,5} \cdot \left(\frac{10}{5 + \xi} \right)^{0.25} \quad (9)$$

Equations (8) and (9) are compared for a range of different levels of damping in Fig.4, in dimensionless form, related to the displacement for 5% damping at a period of $T = 4$ sec, using the EC8 acceleration spectral shape.

For the velocity pulse type ground motion (Fig. 4(b)), the influence of damping in reducing the displacement is much less pronounced than for the “normal” ground motion case of Fig. 4(a). The consequence will be that for a given design displacement and damping, the effective period at peak response for the velocity-pulse ground motion will be smaller than for normal ground motion (follow the dashed lines in Fig.4).

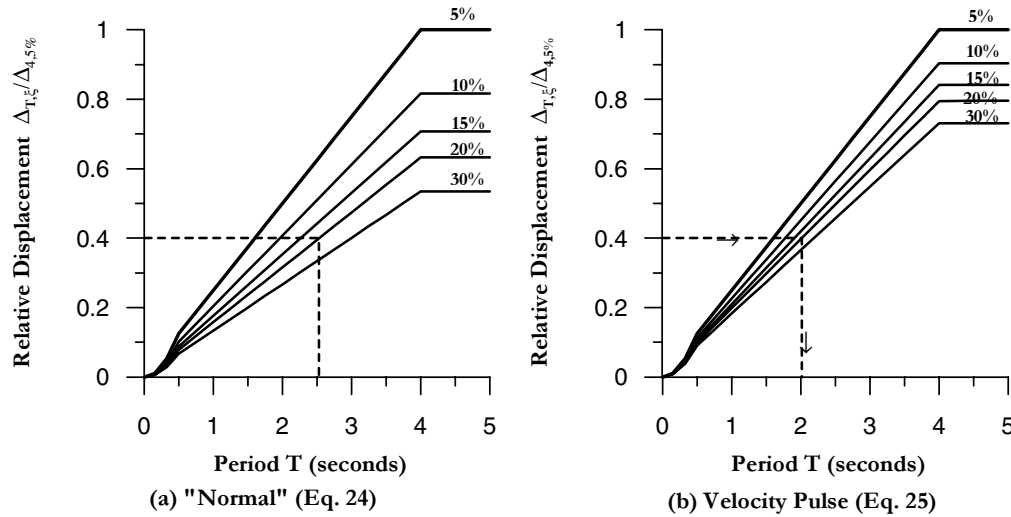


Fig. 4 Influence of Damping on Displacement Response

Non synchronous input

The potential relevance of the spatial variability of the seismic ground motion on the response of bridge structures has been recognized since a long time, however, a relatively little amount of research studies have been developed on the subject. It is accepted that the spatial variability results from the combination

of loss of coherence due to wave propagation, time delay between arrival of wave trains and local filtering due to local site conditions. In a recent comprehensive study [27] it has been pointed out that the accurate determination of the effects of these sources of differential ground motion requires data that are normally beyond the extension of potential studies in real design situations. In this study it has been shown that the ductility demand at the base of the piers increases considerably when the spatial variability is included, even for rather ordinary bridge geometries. As a consequence, it is shown that the probability of collapse may vary of more than one order of magnitude if these phenomena are considered.

In the mentioned paper a procedure to reduce the risk of collapse in presence of potential non-synchronous input is proposed. However, the limited extension of the study, the relatively poor amount of available data and the variability of the results obtained by different researchers [28] and designers in practical cases [14, 15, 16] clearly indicate the need of research and code-oriented studies on this subject.

ASPECTS RELATED TO SEISMIC DESIGN

A displacement – based approach

Fundamental concepts

As discussed in the introduction and as pointed out in several studies [7, 8], a number of fundamental problems can be identified with force-based design. These problems include, among others:

- Invalid assumptions for the relationship between elastic and inelastic displacements;
- Interdependency of strength and stiffness, meaning that stiffness (and hence natural periods, elastic strengths, and strength distribution through the structure) cannot be accurately determined until the structure is fully designed;
- Inadequate representation of variations of hysteretic characteristics of different structural systems;
- Simplistic and inappropriate definition of behavior factors for whole categories of structures, and a lack of appreciation that ductility capacity can vary widely within a structural class – this results has been explicitly described for the case of bridges in [27], where it was shown that a standard design procedure based on a force reduction factor approach cannot guarantee a uniform level of protection;
- Inadequate representation of the influence of foundation flexibility on seismic response;
- Inadequate representation of structural performance of systems where inelastic action develops in different members at different levels of structural response (e.g. bridges with columns of different heights, marginal wharves with ductile piles of different heights, structural wall buildings with walls of different lengths);
- Inadequate representation of structures with dual load paths (e.g. a bridge with an elastic load path involving superstructure action spanning between abutments, and an inelastic load path involving ductile action of the piers).

As discussed in the introduction, several alternative seismic design philosophies have been proposed [10], however, the procedure known as Direct Displacement-Based Design (DDBD) [11], will be briefly addressed here, since it appears to be more intellectually satisfying than the alternatives, and to be best equipped to address the deficiencies of conventional force-based design. Also, it appears to be simpler to apply, and better suited to incorporation in design codes.

The design method is illustrated with reference to figure 5, which considers a SDOF representation of a bridge column, (Fig. 5(a)), though the basic fundamentals apply to all structural types. The bilinear envelope of the lateral force-displacement response of the SDOF representation is shown in Fig. 5(b). An initial elastic stiffness K_i is followed by a post yield stiffness of rK_i .

While force-based seismic design characterizes a structure in terms of elastic, pre-yield, properties (initial stiffness K_i , elastic damping), DDBD characterizes the structure by secant stiffness K_e at maximum

displacement Δ_d (Fig. 5(b)), and a level of equivalent viscous damping ξ_e , representative of the combined elastic damping and the hysteretic energy absorbed during elastic response. Thus, as shown in figure 5(c), for a given level of ductility demand, a structural steel frame building with compact members will be assigned a higher level of equivalent viscous damping than a reinforced concrete frame building, or concrete bridge, designed for the same level of ductility demand, as a consequence of “fatter” hysteresis loops.

With the design displacement at maximum response determined, and the corresponding damping estimated from the expected ductility demand, the effective period T_e at maximum displacement response can be read from a set of displacement spectra for different levels of damping, as shown in the example of figure 5(d). The effective stiffness K_e of the equivalent SDOF system at maximum displacement can be found by inverting the normal equation for the period of a SDOF oscillator to provide

$$K_e = 4\pi^2 m_e / T_e^2 \quad (10)$$

where m_e is the effective mass of the structure participating in the fundamental mode of vibration. From figure 5(b), the design lateral force, which is also the design base shear force, is thus

$$F = V_B = K_e \Delta_d \quad (11)$$

The design concept is thus very simple. Such complexity that exists relates to determination of the “substitute structure” characteristics, the determination of the design displacement, and development of design displacement spectra. Careful consideration is however necessary for the distribution of the design base shear force V_b throughout the structure, and the analysis of the structure under the distributed seismic force.

Elastic Stiffness

In force-based design, the elastic stiffness is required at the start of the design, in order that the elastic periods of the structure can be defined, and also, at a later stage of the design to distribute the total design inertia force to members in proportion to their initial stiffness. It is only recently that it has been recognized that it is inappropriate to use the un-cracked stiffness in period calculations. Now, some recognition is made of the reduction in stiffness caused by cracking, and it is common to use 50% of the gross section moment of inertia ($0.5I_{\text{gross}}$) in estimating section stiffnesses.

More realistically, stiffness can be assessed from the moment-curvature relationship for a section in accordance with the beam equation:

$$EI_{\text{eff}} = M_N / \phi_y \quad (12)$$

where M_N is the nominal moment capacity of the section, and ϕ_y is the yield curvature of the equivalent bilinear representation of the moment-curvature curve. This can be explained with reference to figure 6, which shows a typical moment-curvature relationship together with a bilinear approximation for a 2 m diameter bridge column with 2% longitudinal reinforcement ratio, and light axial load.

It has become accepted by the research community that the most appropriate linearization of moment-curvature relationships is by an initial elastic segment passing through “first yield”, and extrapolated to the nominal flexural strength, M_N , and a post-yield segment connected to the ultimate strength and curvature. “First yield” of the section is defined as the moment, M_y and curvature ϕ'_y when the section first attains the reinforcement tensile yield strain of $\epsilon_y = f_y/E_s$, or the concrete extreme compression fiber attains a strain of 0.002, whichever occurs first. The nominal flexural strength M_N develops when the

extreme compression fiber strain reaches 0.004, or the reinforcement tension strain reaches 0.015, whichever occurs first. Thus, as shown in figure 6(b), the yield curvature is given by:

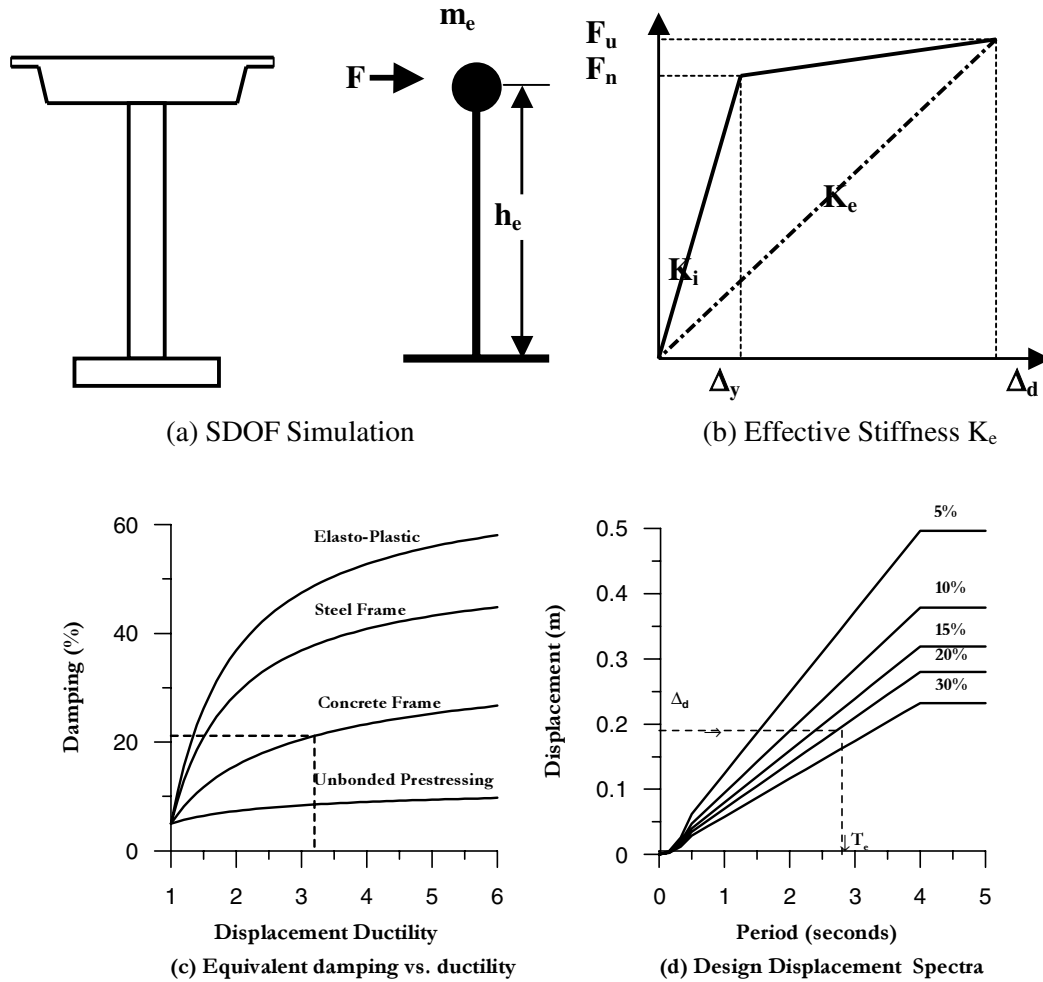


Fig. 5 Fundamentals of Direct Displacement-Based Design

$$\phi_y = \phi'_y M_N / M_y \quad (13)$$

Examination of Eq. (12) reveals that the common design assumption that member stiffness is independent of strength implies that the yield curvature is directly proportional to flexural strength:

$$\phi_y = M_N / EI \quad (14)$$

This assumption is illustrated in figure 7(a). Experimental evidence, and detailed analytical results, indicates that the assumption of stiffness being independent of strength is not valid. In fact, yield curvature is effectively independent of strength, and hence the stiffness is directly proportional to the flexural strength, as is seen from Eq. (12) with ϕ_y a constant. The correct relationship is thus illustrated in figure 7(b). This assertion that section strength and stiffness are directly proportional is tested in figures 6 and 7 for circular bridge columns. Moment-curvature analyses were carried out on circular sections with the following properties:

- Column diameter $D = 2\text{m}$
- Cover to flexural reinforcement 50 mm
- Concrete compression strength $f'_c = 35\text{ MPa}$
- Flexural Reinforcement diameter 40 mm
- Transverse reinforcement: spirals $20\text{mm at } 100\text{mm spacing}$
- Reinforcement yield strength $f_y = 450\text{ MPa}$
- Axial Load Ratio $N_u/f'_c A_g = 0\text{ to } 0.4\text{ (9 levels)}$
- Flexural reinforcement Ratio $\rho_f A_g = 0.005\text{ to } 0.04\text{ (5 levels)}$

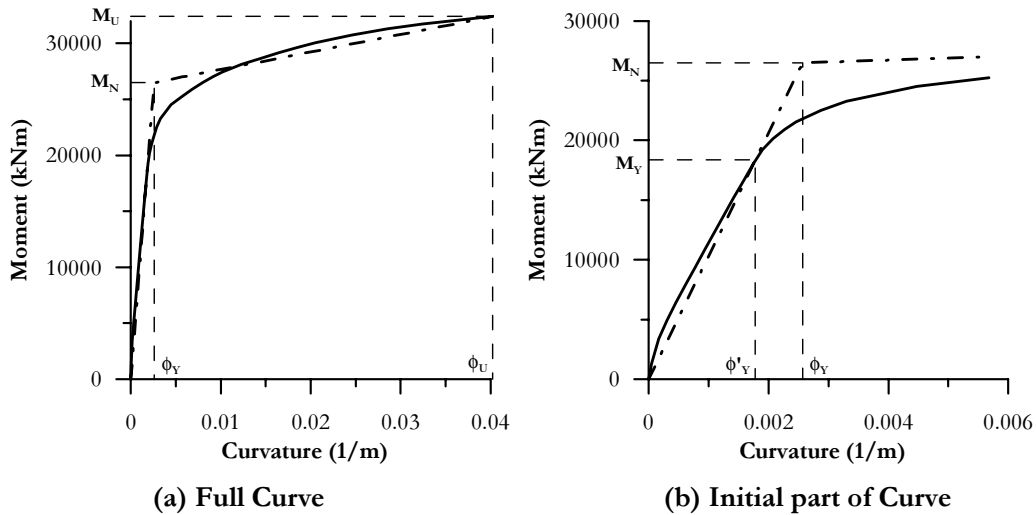


Fig.6 Typical Column Moment-Curvature Relationship [11]

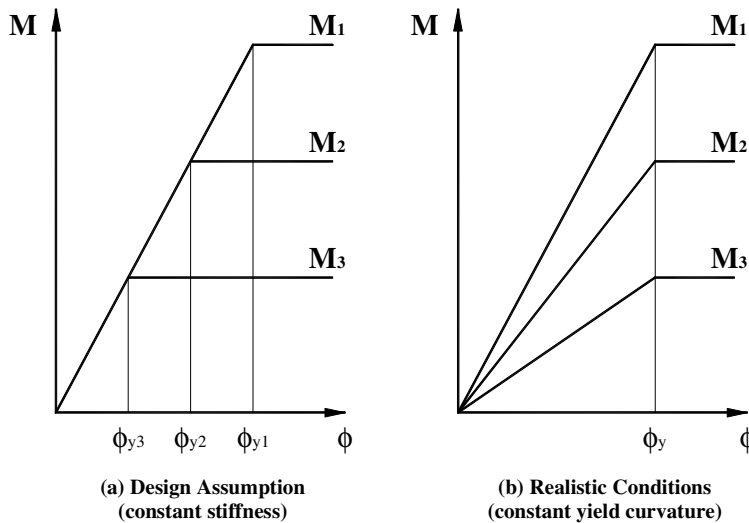


Fig. 7 Influence of Flexural Strength on Moment-Curvature Relationship [8, 11]

A selection of the computed moment-curvature curves is shown in figure 8 for two levels of flexural reinforcement ratio, and a range of axial load ratios. Only the initial part of the moment-curvature curves has been included, to enable the region up to, and immediately after yield to be clearly differentiated. Also shown in figure 8 are the calculated bi-linear approximations for each of the curves. Note that the apparent

over-estimation by the bi-linear representations of the actual curves is a function of the restricted range of curvature plotted.

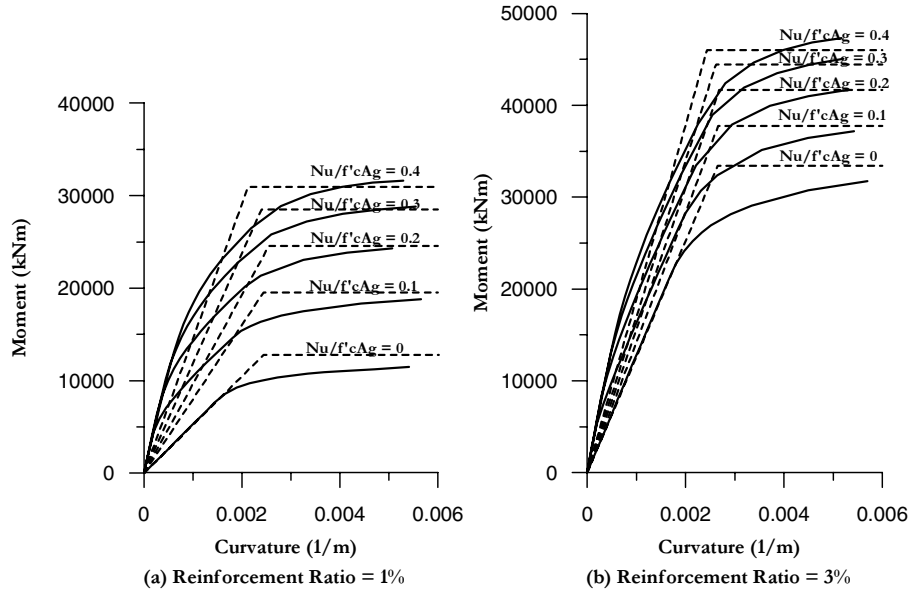


Fig. 8 Selected Moment Curves for Circular Concrete Bridge Columns [11]

Data from the full set of analyses for nominal moment capacity, and equivalent bi-linear yield curvature are plotted in dimensionless form in figure 9. The influence of both axial load ratio and reinforcement ratio on the nominal moment capacity is, as expected, substantial in figure 9(a), with an eight-fold range between maximum and minimum values. On the other hand, it is seen that the dimensionless yield curvature is comparatively insensitive to variations in axial load or reinforcement ratio. Thus the yield curvature is insensitive to the moment capacity. The average value of dimensionless curvature of

$$\phi_{Dy} = \phi_y D / \varepsilon_y = 2.25 \quad (15)$$

is plotted on figure 9(b), together with lines at 10% above and 10% below the average. It is seen that all data with the exception of those for low reinforcement ratio coupled with very high axial load ratio fall within the $\pm 10\%$ limits.

It should be noted that though the data were generated from a specific column size and material strengths, the dimensionless results can be expected to apply, with only insignificant errors, to other column sizes and material strengths within the normal range expected for standard design. The results would not, however apply to very high material strengths (say $f'_c > 50\text{MPa}$, or $f_y > 600\text{MPa}$) due to variations in stress-strain characteristics.

The data in figures 8 and 9 can be used to determine the effective stiffness of the columns as a function of axial load ratio and reinforcement ratio. The ratio of effective stiffness to initial un-cracked section stiffness is thus given by

$$EI_{eff} / EI_{gross} = M_N / (\phi_y EI_{gross}) \quad (16)$$

Results are shown in figure 10 for the ranges of axial load and reinforcement ratio considered. It will be seen that the effective stiffness ratio varies between 0.13 and 0.91. Clearly the assumption that stiffness is a constant for a given section, regardless of strength, is unacceptable.

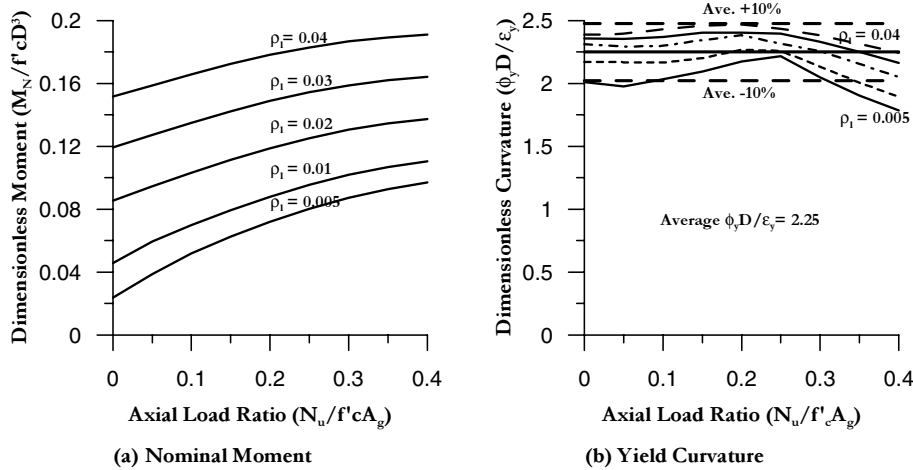


Fig.9 Dimensionless Nominal Moment and Yield Curvature for Concrete Bridge Columns [11]

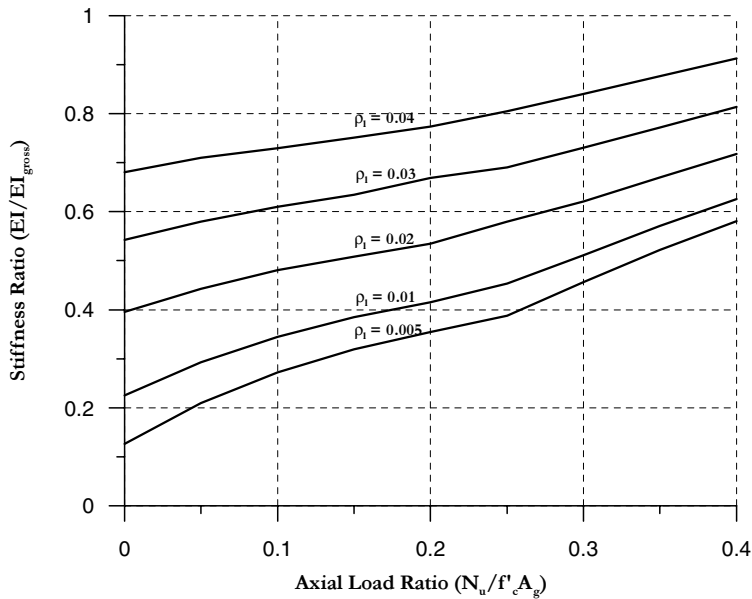


Fig.10 Effective Stiffness of Circular Bridge Columns [11]

Design Displacement

It is comparatively straightforward to compute the design displacement from strain limits. Consider the strain profile at maximum deflection of a simple bridge column under transverse response, defined by the maximum concrete compression strains ϵ_c and the maximum reinforcement tensile strain ϵ_s , for the performance state considered. These will not generally occur simultaneously in the same section, since the neutral axis depth c is fixed by the reinforcement ratio, and the axial load on the section. Consequently there are two possible limit state curvatures, based on the concrete compression and the reinforcement tension respectively:

$$\phi_{mc} = \epsilon_{cm} / c \quad (\text{concrete compression}) \quad (17a)$$

$$\phi_{ms} = \varepsilon_{sm} / (d - c) \quad (\text{reinforcement tension}) \quad (17b)$$

The lesser of ϕ_{mc} and ϕ_{ms} will govern the structural design. The design displacement can now be estimated as:

$$\Delta_{ds} = \Delta_y + \Delta_p = \phi_y H^2 / 3 + (\phi_m - \phi_y) L_p H \quad (18)$$

where ϕ_m is the lesser of ϕ_{mc} and ϕ_{ms} , Δ_y is the yield displacement, H is the column height and L_p is the plastic hinge length.

Ductility Capacity of Bridge Columns

A common assumption of force-based design is that structures of a particular material and class (e.g. concrete; bridge column) have a constant ductility capacity. This is reflected in the specification of a constant force-reduction factor for all structures in that class. Simple evaluation of the basic equations defining ductility capacity reveals that this is inappropriate. An example of the influence of structural geometry on displacement capacity is provided in figure 8, which compares the ductility capacity of two bridge columns with identical cross-sections, axial loads and reinforcement details, but with different heights. The two columns have the same yield curvatures ϕ_y and ultimate curvatures ϕ_u and hence the same curvature ductility factor $\mu_\phi = \phi_u / \phi_y$. Yield displacements, however, may be approximated by

$$\Delta_y = \phi_y H^2 / 3 \quad (19)$$

where H is the effective height, and the plastic displacement $\Delta_p = \Delta_u - \Delta_y$ by

$$\Delta_p = \phi_p L_p H \quad (20)$$

where $\phi_p = \phi_u - \phi_y$ is the plastic curvature capacity. The displacement ductility capacity is thus given by

$$\mu_\Delta = \frac{\Delta_y + \Delta_p}{\Delta_y} = 1 + 3 \frac{\phi_p L_p}{\phi_y H} \quad (21)$$

where L_p is the plastic hinge length.

For circular bridge columns, the plastic hinge length can be expressed as:

$$L_p = 0.08H + 0.022f_y d_b \quad (22)$$

where f_y and d_b are the yield stress (in MPa) and the diameter, of the flexural reinforcement in the plastic hinge region. Using this approach, it is found that the squat column of figure 11(a) has a displacement ductility capacity of $\mu_\Delta = 9.4$, while for the more slender column of figure 11(b), $\mu_\Delta = 5.1$. Clearly the concept of uniform displacement ductility capacity, and hence of a constant force-reduction factor is inappropriate for even this very simple class of structure.

It can easily be shown [8] that the elastic flexibility of the capacity-protected members influences the displacement ductility capacity of the structure, and hence might be expected to influence the choice of force-reduction factor in force-based design. Consider the simple two-column bridge bent illustrated in figure 12. The column bases are connected to the footings by pinned connections, and thus no moments can develop at the base. Plastic hinges are intended to form only at the top of the columns.

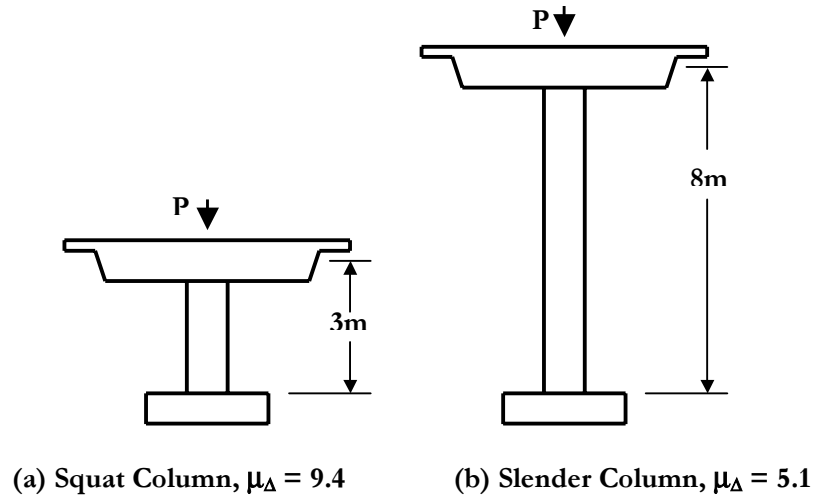


Fig.11 Influence of height on displacement ductility capacity of circular columns ($P = 0.1f'_cA_g$; 2% longitudinal, 0.6% transverse reinforcement) [11]

Consider first the case where the cap beam is assumed to be rigid. The yield displacement under lateral forces F is thus $\Delta_y = \Delta_c$ resulting solely from column flexibility. All plastic displacement originates in the column plastic hinge regions, since the design philosophy requires the cap beam to remain elastic. With a plastic displacement of Δ_p corresponding to the rotational capacity of the column hinges, the structure displacement ductility is

$$\mu_{\Delta_r} = 1 + \frac{\Delta_p}{\Delta_c} \quad (23)$$

Cap beam flexibility will increase the yield displacement to $\Delta_y = \Delta_c + \Delta_b$, where Δ_b is the additional lateral displacement due to cap beam flexibility, but will not result in additional plastic displacement, since this is still provided solely by column hinge rotation. For bent dimensions $H \times L$ and cracked-section moments of inertia for beam and columns of I_b and I_c , respectively, the yield displacement is now

$$\Delta_y = \Delta_c + \Delta_b = \Delta_c \left(1 + \frac{0.5I_c L}{I_b H} \right) \quad (24)$$

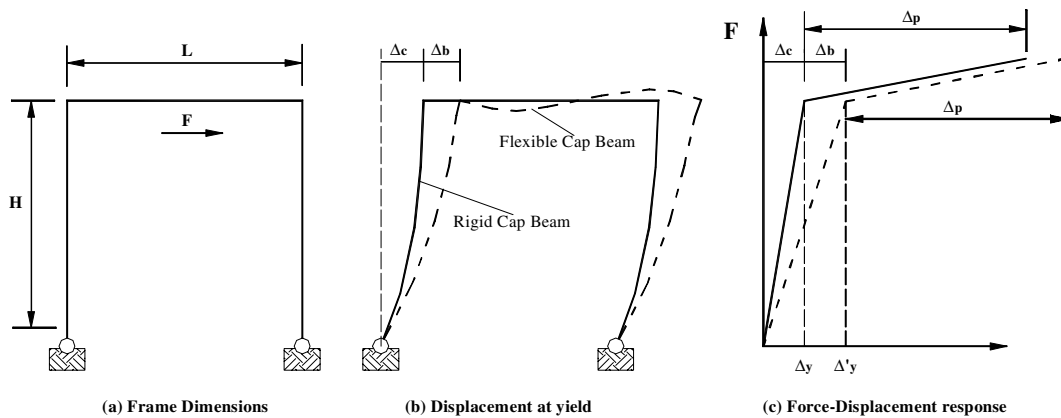


Fig.12 Influence of Cap-Beam Flexibility on Ductility Capacity of Two-Column Bridge Bent [11]

and the structural displacement ductility capacity is reduced to

$$\mu_{\Delta f} = 1 + \frac{\mu_{\Delta r} - 1}{1 + 0.5I_c L / I_b H} \quad (25)$$

As an example, take $L = 2H$, $I_b = I_c$, and $\mu_{\Delta r} = 5$. From Eq. (25) it is found that the displacement ductility capacity is reduced to $\mu_{\Delta f} = 3$. Again it would seem to be inappropriate to use the same force reduction for the two cases. This effect is not included in any design codes, and is rarely adopted in force-based design practice.

Bridges with Dual (Elastic and Inelastic) Load Paths

A more serious deficiency of force-based design is apparent in structures that possess more than one seismic load path, one of which remains elastic while the others respond inelastically at the design earthquake level. A common example is the bridge of figure 13(a), subjected to transverse seismic excitation, as suggested by the double-headed arrows. Primary seismic resistance is provided by bending of the piers, which are designed for inelastic response. However, the abutments are restrained from lateral displacement under transverse response and hence superstructure bending also develops under transverse excitation. Current seismic design philosophy requires the superstructure to respond elastically. The consequence is that a portion of the seismic inertia forces developed in the deck are transmitted to the pier footings by column bending (path 1), and the remainder is transmitted to the abutments by superstructure bending (path 2). An elastic analysis is carried out, and the relative elastic stiffnesses of the two load paths are as indicated by the two broken lines in figure 13(b), which indicates that column flexure (path 1) carries most of the seismic force. A force-reduction factor is then applied, and the forces corresponding to yield displacement are determined.

The inelastic response of the combined resistance of the columns is now shown by the solid line (path 3), and on the basis of the equal displacement approximation it is expected that the maximum displacement is Δ_{\max} , the value predicted by the elastic analysis. If the superstructure is designed on the basis of the force developed in path 2 at the column yield displacement, it will be seriously under-designed, since the forces in this path, which are required to be within the elastic range, continue to rise with increasing displacement. Thus the bending moment in the superstructure, and the abutment reactions are not reduced by column hinging, and a force-reduction factor should not be used in their design.

It is also probable that the maximum response displacement will differ significantly from the initial elastic estimate, since at maximum displacement, the damping of the system will be less than expected, as hysteretic damping is only associated with load path 3, which carries less than 50% of the seismic force at peak displacement response. This will cause an increase in displacements. On the other hand, the higher strength associated with the increased post-yield stiffness of load path 2 may result in reduced displacement demand. Elastic analysis and the force-reduction factor approach give no guidance to these considerations.

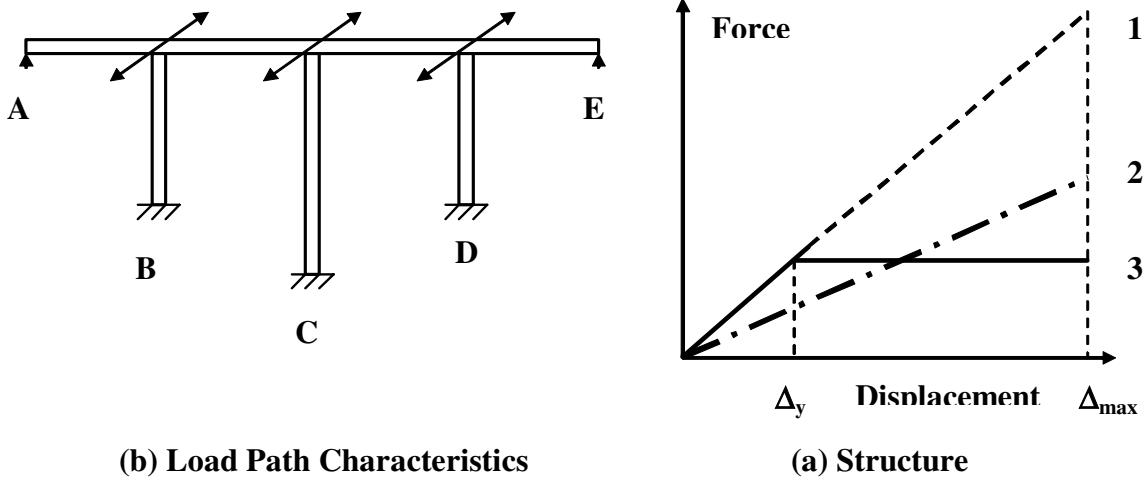


Fig. 13 Bridge with Dual Load Paths under Transverse Response

Design of single-degree-of-freedom bridges

Design Displacement

It is comparatively straightforward to compute the design displacement from strain limits. Consider the simple bridge column under transverse response, of figure 14(a). Two possible reinforced concrete sections, one circular and one rectangular are shown in figure 14(b). The strain profile at maximum displacement response is shown together with the sections. Maximum concrete compression strains ϵ_c and reinforcement tensile strain ϵ_s are developed. The limit strains are ϵ_{cm} and ϵ_{sm} for concrete compression and steel tension respectively, for the performance state considered. These will not generally occur simultaneously in the same section, since the neutral axis depth c is fixed by the reinforcement ratio, and the axial load on the section. Consequently there are two possible limit state curvatures, based on the concrete compression and the reinforcement tension respectively:

$$\phi_{mc} = \epsilon_{cm} / c \quad (\text{concrete compression}) \quad (26a)$$

$$\phi_{ms} = \epsilon_{sm} / (d - c) \quad (\text{reinforcement tension}) \quad (26b)$$

The lesser of ϕ_{mc} and ϕ_{ms} will govern the structural design. The design displacement can now be estimated as:

$$\Delta_{ds} = \Delta_y + \Delta_p = \phi_y H^2 / 3 + (\phi_m - \phi_y) L_p H \quad (27)$$

where ϕ_m is the lesser of ϕ_{mc} and ϕ_{ms} , Δ_y is the yield displacement, H is the column height and L_p is the plastic hinge length (fig.14).

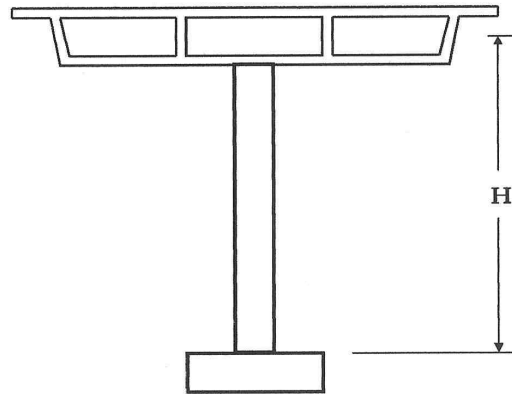
If the limit state has a code-specified non-structural drift limit θ_d the displacement given by Eq. (27) must be checked against

$$\Delta_{d\theta} = \theta h \quad (28)$$

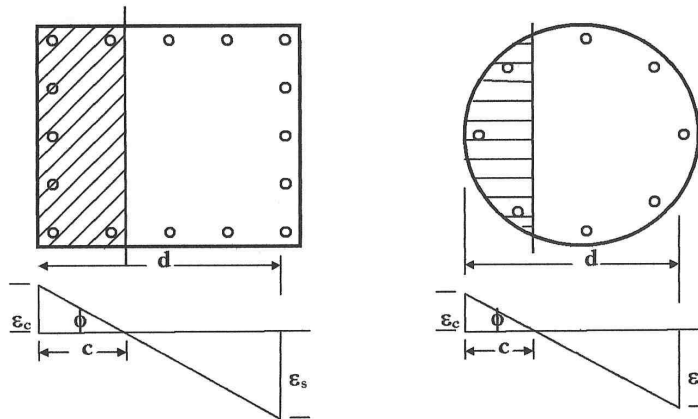
The lesser of the displacements given by Eqs. (27) and (28) is the design displacement.

Note that in many cases the design approach will be to design the structure for a specified drift, and then determine the details to ensure the strain limits are achieved. For example, the limit concrete strain for the damage-control limit state is determined from the transverse reinforcement details. Thus the concrete strain corresponding to the drift limit can be determined by inverting Eqs. (27) and (26a), and the required amount of transverse reinforcement calculated. This simplifies the design process.

Equation (27) requires knowledge of the yield curvature, ϕ_y . As has already been noted in connection with figure 9(b), the yield curvature is a fundamental property of the section, essentially independent of strength, and given in dimensionless form by Eq. (15). It is thus possible to determine the yield displacement, as well as the design displacement, at the start of the design process.



(a) Cantilever Bridge Column



(b) Column Sections and Limit State Strains

Fig.14 Curvatures Corresponding to Limit Strains for a Bridge Pier

Equivalent Viscous Damping

The design procedure requires knowledge of the displacement ductility demand, μ , and of relationships between equivalent viscous damping and displacement ductility demand. From the discussion above, it will be clear that both the design displacement and yield displacement can be calculated at the start of the design process, and hence the displacement ductility demand is also known. For bridge columns, an average relationship between displacement ductility demand and equivalent viscous damping is given by [8]:

$$\xi_d = 5 + 95 \cdot \left(\frac{1 - \mu^{-0.5}}{\pi} \right) \quad (29)$$

where the elastic damping is estimated as 5%.

Multi-degree-of-freedom systems

Like in the case of bridges where a single degree of freedom model is acceptable, the required characteristics are the equivalent mass, the design displacement, and the effective damping. When these have been determined, the design base shear for the substitute structure can be determined. The base shear is then distributed between the mass elements of the real structure as inertia forces and the structure analyzed under these forces to determine the design moments at locations of potential plastic hinges.

Design Displacement

The design displacement (generalized displacement coordinate) is thus given by

$$\Delta_d = \frac{\sum_{i=1}^n (m_i \Delta_i^2)}{\sum_{i=1}^n (m_i \Delta_i)} \quad (30)$$

where m_i and Δ_i are the masses and displacements of the n significant mass locations respectively. For bridges, the mass locations will normally be at the top of the columns, but the superstructure mass may be discretized to more than one mass per span to improve validity of simulation.

Where strain limits govern, the design displacement of the critical member can be determined using the approach outlined in the previous section. Similar conclusions apply when code drift limits apply. For a bridge, the design displacement will normally be governed by the plastic rotation of the shortest column. With knowledge of the displacement of the critical member and the design displacement shape, the displacements of the individual masses are given by

$$\Delta_i = \phi_i \cdot \left(\frac{\Delta_c}{\phi_c} \right) \quad (31)$$

where ϕ_i is the inelastic mode shape, and Δ_c is the design displacement at the critical mass. With bridges, it may not be easy to initially determine a design displacement profile, particularly for transverse response. Fig.15 illustrates two possible configurations out of a limitless possible range. The example of Fig.15 (a) has piers of uniform height, while those in Fig. 15(b) vary in height. The transverse displacement profiles will depend strongly on the relative column stiffnesses, and more significantly, on the degree of lateral restraint provided at the abutment. For each bridge type, three possible transverse displacement profiles are shown, corresponding to an abutment fully restrained against transverse displacement, a completely unrestrained abutment, and one where the abutment is restrained, but has significant transverse flexibility. For the case of figure 15(a), the critical pier will be the central one, and with the appropriate displacement profile chosen, Eq. (30) can be applied directly. For the irregular bridge of figure 15(b) the critical pier may not be immediately apparent, and some iteration may be required. Iteration may also be required for the case of finite flexibility of the abutments for the regular bridge example to determine the relative displacements of abutment and the critical pier. Generally a parabolic displacement shape between abutments and piers can be assumed for initial mode shape. Under longitudinal response, the displacements of all piers will normally be equal, and governed by the shortest pier, and no problems will exist in determining the design displacement.

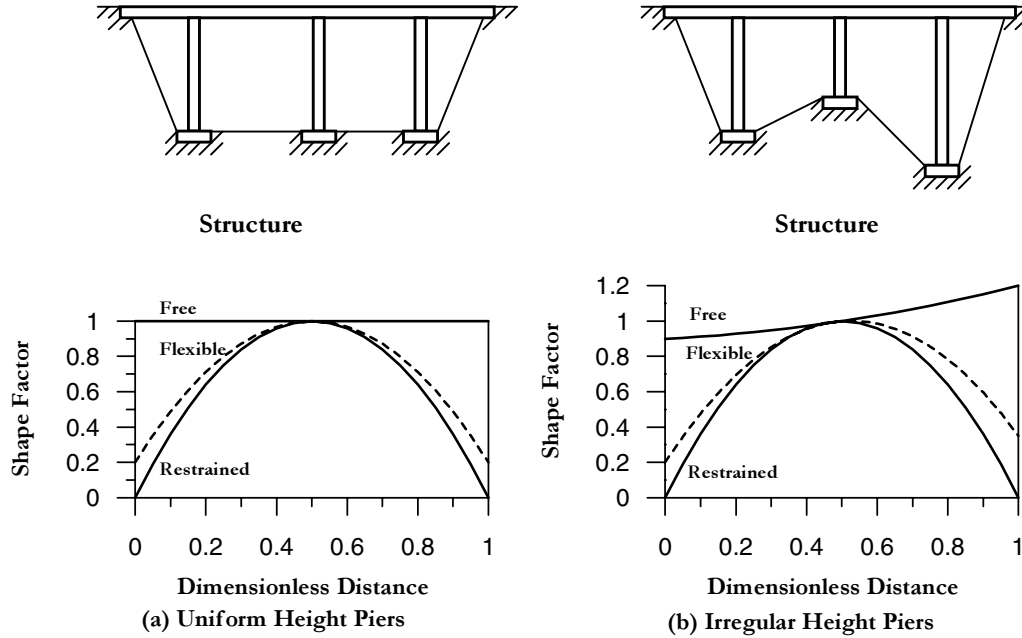


Fig.15 Design Transverse Displacement Profiles for Bridges

Effective Mass

From consideration of the mass participating in the first inelastic mode of vibration, the effective system mass for the substitute structure is

$$m_e = \sum_{i=1}^n (m_i \Delta_i) / \Delta_d \quad (32)$$

Effective Damping

The effective damping depends on the structural system and displacement ductility factor, as illustrated in figures 3 and 4 and Eq.29. In the case of bridges with piers of different heights, as illustrated in Fig.15(b), the piers will have different ductility demands, and an average value, weighted by the shear force in the piers should be used. The system damping is thus:

$$\xi_e = \sum_{j=1}^m (V_j \xi_j) / \sum_{j=1}^m V_j \quad (33)$$

Note that when seismic resistance is provided by dual load paths, with a portion of the seismic inertia forces resisted by superstructure bending, the abutment reactions associated with that action will be included in Eq. (33) and allocated the appropriate level of elastic damping (normally 5%).

Influence of Foundation Flexibility on Effective Damping

Although the influence of foundation flexibility on seismic design can be incorporated into force-based design, albeit with some difficulty, it is rarely considered. Foundation flexibility will increase the initial elastic period, and reduce the ductility capacity corresponding to the strain or drift limit states. It is comparatively straightforward, however, to incorporate the influence of elastic foundation compliance into Direct Displacement-Based Design. If the limit state being considered is strain-limited, then the design

displacement will be increased by the elastic displacement corresponding to foundation compliance (this requires knowledge of the design base moment and shear force, and hence some iteration may be required). If, however, the limit state is defined by code drift limits, there will be no change in the design displacement, thus implying reduced permissible structural deformation.

The second influence relates to the effective damping. Both foundation and structure will contribute to the damping. Consider the force-displacement hysteresis loops of figure 16, where foundation (Δ_f) and structure (Δ_s) components of the peak response displacement $\Delta_d = \Delta_s + \Delta_f$ have been separated for a cantilever bridge pier.

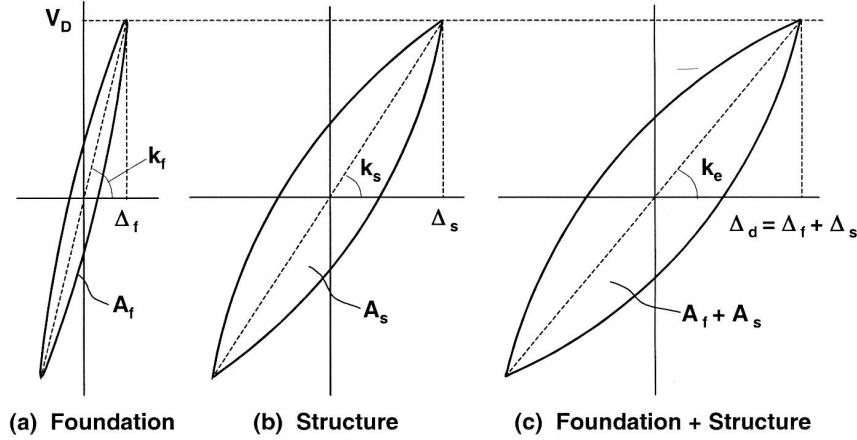


Fig.16 Damping Contributions of Foundation and Structure

The equivalent viscous damping for the foundation and for the structure can be separately expressed as

$$\text{Foundation: } \xi_f = \frac{A_f}{2\pi V_B \Delta_f} \cdot 100\% \quad (34)$$

$$\text{Structure: } \xi_s = \frac{A_s}{2\pi V_B \Delta_s} \cdot 100\% \quad (35)$$

where A_f and A_s are hysteretic areas within the loops (i.e. energy absorbed per cycle) for foundation and structure respectively. As shown in figure 16, the hysteretic area of the combined structure/foundation system will be the sum of the two components, and hence the system equivalent damping will be

$$\text{System: } \xi_e = \frac{A_f + A_s}{2\pi V_B (\Delta_f + \Delta_s)} = \frac{\xi_f \Delta_f + \xi_s \Delta_s}{\Delta_f + \Delta_s} \quad (36)$$

Distribution of Design Base Shear Force

With the design displacement, effective mass, and equivalent viscous damping, the design base shear for the equivalent SDOF structure can then be determined. This must be distributed to the inertia masses in proportion to mass and displacement:

$$F_i = V_B (m_i \Delta_i) / \sum_{i=1}^n (m_i \Delta_i) \quad (37)$$

Analysis of Structure under Design Forces

The structure now needs to be analyzed under the design forces to determine the required flexural strengths at potential plastic hinge locations. In order to be compatible with the *substitute structure* concept that forms the basis of DDBD, member stiffnesses should be representative of effective secant stiffness at the design displacement response. It was noted in relation to Fig 13 and 15 that the inertia forces at the tops of the columns under transverse response would be carried by two mechanisms: elastic bending of the superstructure, and inelastic bending of the columns. The elastic stiffness of the superstructure will be known, but the effective secant stiffnesses of the columns will depend on their final strengths. An iterative solution is necessary, where the stiffness of the critical (shortest) column is assumed, and the stiffnesses of the longer columns determined from the displacement profile, and an assumption of the relative shear demands on the columns. Assuming equal flexural reinforcement in all columns (a logical design choice), and that all columns respond inelastically, then the effective stiffness K_i of column i is related to the effective stiffness K_c of the critical column c by the relationship:

$$K_i = K_c \frac{H_c \Delta_c}{H_i \Delta_i} \quad (38)$$

The bridge is now analyzed under the inertia forces, and the displacement of the critical pier is checked. If the displacement does not equal the design level, the column stiffnesses are increased, or decreased to improve the accuracy. The iterative approach typically converges rapidly.

Influence of seismic intensity on design base shear strength

Force-based and displacement-based design procedures imply significantly different structural sensitivity to seismic intensity [29]. Consider the acceleration and displacement spectra of figure 17, shown for two seismic zones, where the spectral shapes are identical. Two bridges with identical geometry are constructed, one in each of Zones Z_1 and Z_2 . If the bridges were designed by a conventional force-based approach, the fundamental periods would be assumed to be the same, and the design base shears would be related by:

$$V_{b2} = V_{b1} \frac{Z_2}{Z_1} \quad (39)$$

Under direct displacement-based design, the assumption of equal geometry ensures that the yield displacements, and the limit-state design displacements for the two bridges are the same. Hence the ductility, and also the effective damping will also be the same for the two bridges. As may be seen from Fig.17(b), with equal design displacements and damping, the effective periods at design displacement response will be related to the zone intensity by:

$$T_{e2} = T_{e1} \frac{Z_1}{Z_2} \quad (40)$$

From Eqs. (10) and (11), the effective stiffnesses, and hence the design base shears will thus be proportional to the **square** of the seismic intensity:

$$V_{B2} = V_{B1} \left(\frac{Z_2}{Z_1} \right)^2 \quad (41)$$

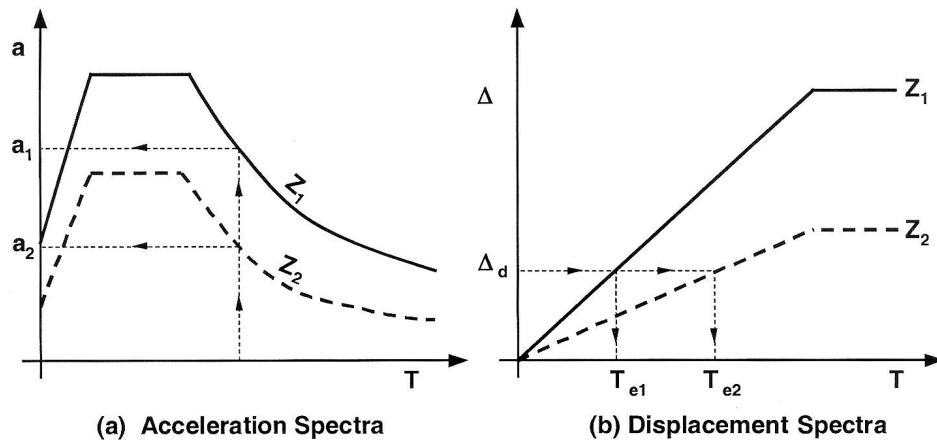


Fig.17 Influence of Seismic Intensity on Design Base Shear Force [29]

It should be noted that the same conclusion would be obtained from force-based design if the design calculations were iterated based on successive estimates of stiffness, attempting to achieve the same displacement ductility.

CONCLUSIONS

Usually, state of the art papers may have no conclusions, since the objective is a critical evaluation of the scientific and professional trends, necessarily spread throughout the text. However, it is here felt appropriate to note how recent experience and research developments on bridge response, design, assessment and strengthening points unanimously towards the same line of thoughts and future developments.

It is evident that displacement demand and capacity are being fully recognized as the key design parameters, but the full picture of coherent consequences still has to be thoroughly explored and exploited.

Clearly, capacity design principles will maintain their fundamental role of protecting brittle failure modes in favor of mechanisms able to provide significant displacement capacities and effective energy dissipation. In this picture, strength evaluations will be used essentially to compare different damage and failure modes, and therefore to impose (for new design) or to assess (for existing bridges) the post elastic mechanism.

Various forms of isolation, such as controlled ground layers (following the line traced in the design of the Rion bridge), rocking at the foundation level, simple or multiple rocking along the height of the piers, or more conventional deck isolation obtained inserting appropriate devices between pier and deck are likely to become standard practice.

The emphasis on displacement will require important revision of the representation of the input ground motion, to describe the structure displacement demand as a function of input parameters such as magnitude, source mechanism, hypocenter depth, distance between the site and the fault plane. The effects of non-synchronous input ground motions may also find different logic of representation, since they appear to be more closely related to displacement than to acceleration demand.

The philosophies of assessment and strengthening of existing bridges (and more generally of all kinds of structures) will be consequently strongly affected, since weaker element will become irrelevant provided that will show adequate displacement capacity.

Similarly, analytical tools may be refocused and design and application of devices to reduce and control the response may be rethought (this issues have not been discussed in this paper for reason of space).

In the seventies, the concepts of ductility and capacity design started being spread through the earthquake engineering scientific community, initiating a sort of revolutionary process that took approximately thirty years to reach full maturity in the state of practice and design codes. It is now felt that new revolutionary seeds are being spread, that may possibly take a few decades to become, in turn, state of practice.

To be part of the process is an exciting commitment.

ACKNOWLEDGEMENTS

A state of the art report is always an attempt of a critical collection of recent work and opinions of leading researchers and professionals, implicitly acknowledged in the references. In this specific case the author wishes to add that the ground and context of development of the thoughts expressed in this paper have to be found in the profitable meetings of several fib task groups (see for example [10]) and in the continuous pleasant and stimulating confrontation with Nigel Priestley, now lasting for more than fifteen years and currently additionally motivated by the preparation of a new book [30], which has been a fundamental reason to explore most of the material discussed in this paper.

REFERENCES

1. Priestley, M.J.N., F. Seible, and G.M. Calvi, *Seismic Design and Retrofit of Bridges*, John Wiley and Sons, New York, 1996
2. Seismic Design and Retrofit of Reinforced Concrete Bridges, Proceedings of the International Workshop held in Bormio, Univerità degli Studi di Pavia, Italy, 1991.
3. Seismic Design and Retrofitting of Reinforced Concrete Bridges, Proceedings of the International Workshop, Queenstown, University of Canterbury, New Zealand, 1994.
4. Kawashima, K., Seismic design and retrofit of bridges, Keynote address, 12th World Conference on Earthquake Engineering, Auckland, 2000
5. Newmark, N.M., and W.J. Hall, Procedures and criteria for earthquake resistant design, building practice for design mitigation, Building Science Series 45, National Bureau of Standards, Washington, 1973, 209-236
6. Park R., and T. Paulay, *Reinforced Concrete Structures*, Jonh Wiley & Sons, 1975
7. Priestley, M.J.N., Myths and Fallacies in Earthquake Engineering – Conflicts Between Design and Reality, *Bulletin of the NZ National Society for Earthquake Engineering*, Vol.26., No.3, 1993, 329–341
8. Priestley, M.J.N., *Myths and Fallacies in Earthquake Engineering, Revisited*, The 9th Mallet Milne Lecture, 2003. IUSS Press, Pavia, 2003
9. ICBO, *Uniform Building Code UBC'97*, International Conference of Building Officials, Whittier, 1997
10. fib TG 7.2, *Displacement-based seismic design of reinforced concrete structures*, fib Bulletin 25, Lausanne, 2003
11. Priestley, M.J.N. and G.M. Calvi, Direct displacement-based seismic design of concrete bridges, ACI International Conference on Seismic Bridge Design and Retrofit, La Jolla, 2003

12. Gulkan, P. and M. Sozen, Inelastic Response of Reinforced Concrete Structures, *ACI Journal*, Vol. 71, 1974, 604-610
13. Shibata, A., and M. Sozen, Substitute Structure Method for Seismic Design in Reinforced Concrete, *Journal of the Structural Division*, ASCE, Vol. 102, No.12, 3548–3566
14. Teyssandier, J.P., The Rion Antirion bridge design and construction, ACI International Conference on Seismic Bridge Design and Retrofit, La Jolla, 2003
15. Pecker, A., Aseismic foundation design process, lessons learned from two major projects: the Vasco de Gama and the Rion Antirion bridges, ACI International Conference on Seismic Bridge Design and Retrofit, La Jolla, 2003
16. Priestley, M.J.N. and G.M. Calvi, Strategies for repair and seismic upgrading of Bolu Viaduct 1, Turkey, *Journal of Earthquake Engineering*, SP1, Vol. 6, 2002, 157-184
17. 1999 Kocaeli, Turkey, Earthquake Reconnaissance Report, *Earthquake Spectra*, Supplement to Vol. 16, 2000
18. Faccioli E., R. Paolucci and V. Pessina, Engineering assessment of seismic hazard and long period ground motions at the Bolu viaduct site following the November 1999 earthquake, *Journal of Seismology*, Vol. 6, No. 3, 2002, 307–327
19. Calvi, G. M., D. Bolognini, P. Ceresa, C. Casarotti and F. Auricchio, Effects of axial force variation on the seismic response of bridges isolated with friction pendulum systems, *Journal of Earthquake Engineering*, accepted for publication
20. Somerville, P., Characterization of near fault ground motions for design, ACI International Conference on Seismic Bridge Design and Retrofit, La Jolla, 2003
21. Bommer, J.J., A.S. Elnashai, and A.G. Weir, Compatible Acceleration and Displacement Spectra for Seismic Design Codes, Proc.12th WCEE, Auckland, Paper 0207, 2000
22. Faccioli, E., R. Paolucci, and J. Rey, Displacement Spectra for Long Periods, *Earthquake Spectra*, accepted for publication
23. CEN, EC8, *Design Provisions for Earthquake Resistance of Structures*, Pub. ENV-1998-2, Comite Europeen de Normalization, Brussels, Belgium, 1998
24. Ambraseys, N. and J. Douglas, Reappraisal of the effect of vertical ground motions on response, ESEE Report No. 00-4, Imperial College, London, 2000
25. Ghobarah, A. and A.S. Elnashai, Contribution of vertical ground motion to the damage of RC buildings, Proceedings of the Eleventh European Conference on Earthquake Engineering, Balkema, Paris, 1998
26. Elnashai, A.S. and A.J. Papazoglou, Procedure and spectra for analysis of RC structures subjected to strong vertical earthquake loads, *Journal of Earthquake Engineering*, 1(1), 1997, 121-155
27. Pinto, P.E., A. Lupoi, P. Franchin and G. Monti, Seismic design of bridges accounting for spatial variability of ground motion, ACI International Conference on Seismic Bridge Design and Retrofit, La Jolla, 2003
28. Sextos, A.G., K.D. Pitilakis and A.J. Kappos, Inelastic dynamic analysis of RC bridges accounting for spatial variability of ground motion: site effects and soil–structure phenomena, *J. of Earthquake Engineering and Structural Dynamics*, Vol. 32, 2003, 607–652
29. Priestley, M.J.N., Performance Based Seismic Design, Keynote address, 12th World Conference on Earthquake Engineering, Auckland, 2000
30. Priestley, M.J.N., G.M. Calvi and M.J. Kowalsky, *Direct Displacement-Based Seismic Design of Structures*, IUSS Press, Pavia, in preparation